Applied Geochemistry 143 (2022) 105389

Contents lists available at ScienceDirect

Applied Geochemistry

journal homepage: www.elsevier.com/locate/apgeochem

Sorption mechanism of Fe(II) on illite: Sorption and modelling

Ping Chen [a,b,*], Luc Robert Van Loon [a], Maria Marques Fernandes [a], Sergey Churakov [a,b]

[a] Paul Scherrer Institut, Laboratory for Waste Management, 5232, Villigen, PSI, Switzerland
[b] Institute of Geological Science, University of Bern, Switzerland

ARTICLE INFO

Editorial handling by: Dr Johannes Lützenkirchen

Keywords:
Sorption edge
Sorption isotherm
2 SPNE SC/CE sorption Model

ABSTRACT

Different countries consider clay formations as potential host rocks for a deep geological disposal of radioactive waste. Minor amounts of Fe(II), which is an important reducing agent in geochemical processes, are typically present in illite, which is a one of the major clay minerals present in different argillaceous rocks. On other hand, the corrosion of nuclear waste casks may act as sources of Fe(II) over time. The presence of Fe(II) in clay minerals may control the behavior of redox sensitive radionuclides such as ^{99}Tc, ^{75}Se and U, whose sorption, solubility and migration are largely affected by their redox state, which is affected by the redox potential in the environment. Thus, a quantitative description of Fe(II) sorption on clay minerals such as illite, is important to understand subsequent reactions with redox sensitive radionuclides. In this study, the sorption of Fe(II) on illite was investigated in batch experiments, including sorption edge and sorption isotherms measurements under anoxic condition. A 2 SPNE SC/CE (2 sites protolysis non-electrostatic surface complex/cation exchange) sorption model extended to account for the surface oxidation of sorbed Fe(II) was used to model the sorption data with geochemical modelling code PHREEQC. Three models (A, B, C) with increasing level of complexity were tested. The model A, in which only Fe(II) interact with illite, fit the experimental data not satisfactorily. This model was modified to include oxidation of surface complexes (Model B) and precipitation of iron bearing phases (Model C). The modified models showed that most of the sorbed Fe(II) was oxidized at pH below 6.5. At pH above 6.5, the oxidized surface complexes either react with water forming surface iron hydroxides or precipitate as hematite, although presence of these could not be confirmed by X-ray diffraction measurements. These sorption processes could be used to couple with redox sensitive radionuclides in future reactive transport research.

1. Introduction

Different countries consider clay formations as potential host rocks for a deep geological disposal of radioactive waste (Altmann, 2008; Andra, 2005; Lázár and Máthé, 2012; Nagra, 2002; Ondraf/Nirond, 2001). Clay minerals are important components of argillaceous rocks and backfill materials used in designs of waste repositories. Clay minerals may contain significant amounts of Fe (II) (Baeyens and Bradbury, 1997; Baeyens et al., 1985; Bradbury and Baeyens, 1999; Jaisi et al., 2005; Keeling et al., 2000; Kefas et al., 2007; Mogyorosi et al., 2003; Nayak and Singh, 2007; Poinssot et al., 1999), which is an important reducing agent in natural clays rocks. Iron containing clay minerals may control the long-term fate of redox sensitive radionuclides such as ^{75}Se and ^{99}Tc (De Cannière et al., 2010; Jaisi et al., 2009; Ma et al., 2019; Tsarev et al., 2016). Their speciation was demonstrated to play a significant role in reactions with redox sensitive nuclides. For instance, the following affinity series for heterogeneous Tc(VII) reduction by different Fe(II) species was observed: aqueous Fe(II) ≈ adsorbed Fe(II) in phyllosilicates < structural Fe(II) in phyllocilicates < Fe(II) adsorbed on Fe (III) oxides (Peretyazhko et al., 2008). Fe(II)-bearing minerals are known to reduce Tc(VII) to hydrous TcO_2-like phases (McBeth et al., 2011). In the study of Brookshaw et al., TcO_4^-, UO_2^{2+} and NpO_2^+ could be removed from solution by microbially reduced biotite and chlorite, and its reactivity was associated with redox cycling of the small fraction of Fe in these minerals (Brookshaw et al., 2015). On other hand, the corrosion of nuclear waste cannisters may act as a source of Fe(II) over time and not much is known about its behavior once it encounters the host clay rocks, in which clay minerals are the main component. Further, adding Fe(II) is a potential remediation technology for soils and sediments contaminated by redox sensitive nuclides. Therefore, it is important to have a comprehensive understanding of iron adsorption on clay minerals, and to develop quantitative sorption models, as part of models that describe and predict the long-term fate of redox sensitive nuclides for the safety assessment of radioactive waste repositories and/or

* Corresponding author. Paul Scherrer Institut, Laboratory for Waste Management, 5232, Villigen, PSI, Switzerland.
E-mail address: ping.chen@students.unibe.ch (P. Chen).

https://doi.org/10.1016/j.apgeochem.2022.105389
Received 4 August 2021; Received in revised form 13 June 2022; Accepted 30 June 2022
Available online 9 July 2022

remediation of polluted soils and sediments.

The redox properties of iron in clay minerals such as smectites (Gorski et al., 2012, 2013; Hofstetter et al., 2006), nontronite (Jaisi et al., 2008; Neumann et al., 2013) and montmorillonite (Latta et al., 2017; Tsarev et al., 2016) have been widely investigated. Its redox behavior in illite, especially the reactivity towards redox sensitive radionuclides, is largely unknown and needs a better understanding. In this study, a sorption edge and sorption isotherms were measured in batch experiments in order to obtain a comprehensive understanding of Fe(II) uptake mechanisms on illite. The two site protolysis non-electrostatic complexation and cation exchange (2SPNE SC/CE) sorption model, which was demonstrated to successfully and quantitatively explain the sorption mechanism of numerous cations (Bradbury and Baeyens, 2009a, b; Bradbury and Baeyens, 1997, 2005), was applied to model the sorption edge and sorption isotherm of Fe(II) on purified homoionic Na-illite with the help of PHREEQC. The model was further extended to take into account oxidation of surface complexes. Further XRD (X-ray diffraction) measurements were performed to verify whether precipitates were formed on the surface.

2. Materials and methods

2.1. Illite preparation

The illite used in this study was Illite du Puy (IDP) from Le Puy-en-Velay (France) (Gabis, 1958). Samples of illite were treated with a standard purification protocol described in Bradbury (Baeyens and Bradbury, 2004). The protocol described in Glaus et al. (2010) was applied to remove Ca-phases. The illite was equilibrated with a 1 M NaCl solution (solid to liquid ratio was 50 g/L) by stirring with a magnetic stirrer for 4 h. The solution was buffered at pH 3.5 by a formic acid/-formate buffer. After settling down of the illite particles for 24 h, the supernatant was replaced by a fresh 1 M NaCl electrolyte, and the procedure was repeated until no more Ca^{2+} could be extracted by this acid buffer (normally 7–8 times and verified by Ion Chromatography measurement of the supernatant). Then the suspension was washed with pure 1 M NaCl for 3 times to remove the residual acid buffer. After removing the NaCl by dialysing the suspension against de-ionized water, the illite was freeze-dried. The dried illite was stored under atmospheric conditions. All chemicals used were of suprapur grade quality.

2.2. Batch sorption

The illite suspension was prepared by adding about 3 g of pretreated illite (see section 2.1) to 100 mL of 0.1 M NaCl. All sorption experiments were performed in a glovebox under a controlled N_2 atmosphere (O_2 < 0.1 ppm) at 25 ± 1 °C. Before being transferred into the glovebox, the illite suspension and aqueous solutions were deoxygenated by heating to 60 °C and bubbling N_2 through the solutions for at least 2 h. Tracer ^{55}Fe was purchased from Eckert & Ziegler Isotope Products, CA. Three $FeCl_2$ stock solutions (10^{-3} M, 10^{-4} M and 10^{-5} M) were prepared by dissolving given amounts of $FeCl_2$● $4H_2O$ in 0.1 M NaCl solution. These stable $FeCl_2$ stock solutions together with ^{55}Fe tracer were first reduced in an electrochemical cell (Eh = −0.65 V vs SHE) as depicted in (Aeschbacher et al., 2010), to ensure all iron was in a reduced state, that is Fe(II). The cell consisted of a glass vessel closed with a teflon cover, a glassy carbon working electrode (Sigradur G, HTW, Germany), an Ag/AgCl reference electrode and a coiled wire platinum auxiliary electrode (Bioanalytical Inc., West Lafayette, IN) (Aeschbacher et al., 2010).

Sorption edge measurements were carried out at trace Fe(II) concentrations (10^{-7} M) with 0.1 M NaCl as the background electrolyte (about 8 × 10^{-10} M Fe-55 in each tube). The solid to liquid ratio was about 1 g/L^{-}. In order to fix the pH at a specific value, several buffers were used at a concentration around 0.002 M. The following pH buffers were used: sodium acetate for pH 3.5–4.5, MES (2-(N-morpholino) ethanesulfonic acid) for pH 5.5–6.5, MOPS (3-(N-morpholino) propanesulfonic acid) for pH 7.0–7.5, TRIS (tris (hydroxymethyl)aminomethane) for pH 8.0–8.5 and CHES (N-cyclohexyl-2-aminoethanesulfonic acid) for pH 9.0–9.5. These buffers were observed not to affect the interaction between Fe(II) and the clay mineral surface (Soltermann et al., 2014b). Illite suspensions were contacted with ^{55}Fe tracered and electrochemically reduced Fe(II) solutions in 25 mL centrifuge tubes (polypropylene). After shaking the systems end-over-end for three days, the suspensions were centrifuged in the glove box at 35 000 rpm for 1 h (Beckman-Coulter Ultra-centrifuge, Beckman Coulter, Krefeld, Germany). The ^{55}Fe activity in the supernatant was measured by liquid scintillation counting (Tri-Carb 2750 TR/LL liquid scintillation counter, Canberra Packard, Schwadorf, Austria) using Ultima Gold AB (PerkinElmer, America) as scintillation cocktail. The Fe(II) distribution ratio was obtained by applying the following equation (1).

$$R_d = \frac{c_{in} - c_{eq}}{c_{eq}} \cdot \frac{V}{m} \left(L \cdot kg^{-1}\right) \quad (1)$$

where c_{in} and c_{eq} are the total initial and the equilibrium Fe(II) concentrations, respectively, V is the volume of the liquid phase and m is the mass of solid. The sorption edge was plotted as the logarithm of the distribution ratio R_d as function of pH (Baeyens and Bradbury, 1997; Bradbury and Baeyens, 1997). The sorption isotherm was measured following almost the same protocol, except that the pH was fixed at a specific value and the Fe(II) concentrations were varied from 10^{-7} M to 10^{-3} M (the tracer is the same as sorption edge). In this study, isotherms were measured at three pH conditions, pH 5.0, pH 5.5 and pH 6.5. Two datasets were used for the sorption model development, the other was applied to test and verify the model. The calculation of the uncertainties of R_d and the uncertainties of sorbed Fe are shown in detail in the Supporting Information S1 and Table S1.

Samples were prepared separately for XRD measurement to make sure whether a Fe-precipitate was formed. These samples were prepared under the same condition as the sorption edge at pH 6.86 and pH 8.68, and as the sorption isotherm at 2 × 10^{-4} M Fe(II), except that more illite was added (7.5 g/L), i.e. about 0.3 g. Samples were sealed and stored under N_2 for transfer to the XRD facility (the PANalytical X'Pert Pro). XRD patterns were recorded with an Empyrean diffractometer using Cu Kα radiation (λ = 1.5406 Å) under a 45 kV working voltage and 40 mA current at room temperature. Step scanning was performed with an angular resolution of 0.01° at 25 s counting time.

2.3. Sorption model

The two-site protolysis non-electrostatic surface complexation and cation exchange (2SPNE SC/CE) sorption model was developed by Baeyens and Bradbury (1997) to describe Ni and Zn sorption on Na-montmorillonite (Bradbury and Baeyens, 1997). Later on, it has been widely used to describe the uptake of various metals on clay minerals (Bradbury and Baeyens, 1999, 2002, 2006, 2009b, 2011; Bradbury et al., 2005; Poinssot et al., 1999). A mechanistic study of Fe(II) sorption on montmorillonite, whose structure is in many aspects similar to illite, was performed by Soltermann et al. (2014a; 2014b). In this model, a combination of surface complexation at the amphoteric surface hydroxyl groups (≡SOH sites) and cation exchange on the planar sites is used to explain the cations uptake. The protolysis behavior of clay minerals is described by two types of weak sites (≡S^{w1}OH and ≡S^{w2}OH), which have the same site capacity (4.0 × 10^{-4} mol kg^{-1}) but different protolysis constants, together with one type of strong site (≡S^{S}OH) with a higher affinity but a lower capacity, which shows the same protolysis constant as the ≡S^{w1}OH sites. The properties of purified Na-illite were fully characterized by Baeyens and Bradbury (2004). Values for the cation exchange capacity (CEC), the surface hydroxyl group capacity and protolysis constants, which were fixed parameters in the sorption model, are listed in Table 1. The model was implemented in the

PHREEQC software (version 3.4.8 and database is the phreeqc.dat) that was used to perform the modelling. The input data is available in the support information Text S1.

3. Results and discussion

Fig. 1 shows Fe(II) sorption on illite as a function of pH, and comparison with sorption on montmorillonite (Soltermann et al., 2013; Soltermann et al., 2014a, 2014b), and the sorption isotherm at pH 5.0 ± 0.1, pH 5.5 ± 0.1 and pH 6.5 ± 0.1. As shown in Fig. 1a, the sorption edge data is similar to sorption on montmorillonite (or more precisely between the Wyoming montmorillonite and the Texas montmorillonite). R_d is constant at pH < 4, increases from pH 4 to pH 7 and reaches a plateau above pH 7. Interesting point is the sorption edge on IDP (Illite du Puy) is between the Texas montmorillonite (or the synthetic iron free montmorillnote) and the Wyoming montmorillonite. As observed in Soltermann et al. (2014a), sorbed Fe(II) was oxidized on Fe(III)-rich montmorillonite, whose structural Fe contents for STx and SWy are 0.5 wt%, 2.9 wt%, while that for illite is 5.18 wt% (Murad and Wagner, 1994). This remind a similar oxidation is possible and will be discuss detially below. The three isotherms at different pH values are shown in Fig. 1b. The isotherm sorption at pH 5.0 ± 0.1 and pH 6.5 ± 0.1 are used to achieve the best fit parameters, Isotherm sorption at pH 5.5 ± 0.1 is used to test and verify these parameters.

In water under reducing conditions Fe^{2+} is expected to form $FeOH^+$, $Fe(OH)_2$, and $Fe(OH)_3^-$ aqua complexes. Under oxidizing conditions, Fe^{2+} oxidizes to Fe^{3+}, and further reacts with water to form $Fe(OH)_2^+$, $Fe(OH)_3$ and $Fe(OH)_4^-$. Similar hydrolysis reactions are expected for Fe^{2+} adsorbed on the illite surface. So, the Fe^{2+} behavior in reducing conditions and in conditions having a redox potential according to equation (6) (which will be discussed in detail below) was calculated with PHREEQC and is given in Fig. 2. Fe speciation with the formation of a hematite precipitate is shown in Fig. S1 in the Supporting Information. Under the redox potential being considered, Fe^{2+} is the dominant species at pH < 6, and becomes gradually oxidized above pH 6. Oxidized Fe predominantly exists as $Fe(OH)_3$ at pH 7–9, with small amounts of $Fe(OH)_2^+$. $Fe(OH)_4^-$ gradually becomes predominant from pH 9. While Fe^{2+} and $FeOH^+$ is dominant from pH 2 to 9 and pH 9 to 10, respectively, if redox reactions are not taken into account. In this study, the sorption edge measurements of Fe(II) on illite were performed at a pH range from 2 to 10. So, the dominant Fe species are Fe^{2+}, $Fe(OH)_3$, and $Fe(OH)_4^-$, if oxidation was taken into account; or Fe^{2+} and $FeOH^+$ if oxidation was not taken into account.

Table 1
Cation exchange capacities, surface hydroxyl group capacities and protolysis constants of illite (Baeyens and Bradbury, 2004, Bradbury and Baeyens, 2009a) and hydrolysis reactions of Fe^{2+}.

Site types	Site capacities
$\equiv S^SOH$	2.0×10^{-3} mol/kg
$\equiv S^{W1}OH$	4.0×10^{-2} mol/kg
$\equiv S^{W2}OH$	4.0×10^{-2} mol/kg
CEC	2.25×10^{-1} eq/kg
Protolysis reactions	Log $K_{protolysis}$
$\equiv S^SOH + H^+ \leftrightarrow \equiv S^SOH_2^+$	4.0
$\equiv S^SOH \leftrightarrow \equiv S^SO^- + H^+$	−6.2
$\equiv S^{W1}OH + H^+ \leftrightarrow \equiv S^{W1}OH_2^+$	4.0
$\equiv S^{W1}OH \leftrightarrow \equiv S^{W1}O^- + H^+$	−6.2
$\equiv S^{W2}OH + H^+ \leftrightarrow \equiv S^{W2}OH_2^+$	8.5
$\equiv S^{W2}OH \leftrightarrow \equiv S^{W2}O^- + H^+$	−10.5
Hydrolysis reactions	Log ^{OH}K
$Fe^{2+} + H_2O \leftrightarrow Fe(OH)^+ + H^+$	−9.1 ± 0.4
$Fe^{2+} + 2\ H_2O \leftrightarrow Fe(OH)_2^0 + 2\ H^+$	−20.6 ± 1.0
$Fe^{2+} + 3\ H_2O \leftrightarrow Fe(OH)_3^- + 3\ H^+$	−34.6 ± 0.4

3.1. Sorption model A: Fe(II) – illite interaction

The CEC, surface hydroxyl group sites density and protolysis constants of illite were fixed at values given by Baeyens and Bradbury (Baeyens and Bradbury, 2004, Bradbury and Baeyens, 2009a). The cation exchange reaction between Fe(II) and Na^+ was written as following (Gaines and Thomas, 1953):

$$Fe^{2+} + 2Na^+ - \text{Illite} \leftrightarrow Fe^{2+} - \text{Illite} + 2Na^+$$

The selectivity coefficient (K_c) was defined as:

$$^{Fe^{2+}}_{Na^+}K_c = \frac{N_{Fe^{2+}}}{(N_{Na^+})^2} \cdot \frac{\{Na^+\}^2}{\{Fe^{2+}\}} \quad (2)$$

where $N_{Fe^{2+}}$ and N_{Na^+} are equivalent fractional occupancies, defined as the equivalents of Fe (or Na) sorbed per kilogram of illite divided by the CEC, and {} are the activities of cations in solution.

Two types of "weak surface sites" and one "strong site" are considered. The corresponding reactions are shown in equation (3).

$$\equiv S^{S,W1,W2}OH + Fe^{2+} \leftrightarrow \equiv S^{S,W1,W2}OFe^+ + H^+$$

The reaction equilibrium constant (K_M) for these reactions is defined as:

$$K_{Fe2+} = \frac{\left[\equiv S^{S,W1,W2}OFe^+\right] \cdot \{H^+\}}{\left[\equiv S^{S,W1,W2}OH\right] \cdot \{Fe^{2+}\}} \quad (3)$$

where { } are the activities of the aqueous species and [ ] are the concentration of the surface complexes and hydroxyl groups at the strong and weak sites.

Reaction equilibrium constants without an electrostatic term were applied. Firstly, the equilibrium constants of cation exchange and complexation with the strong site were optimized by modelling of the sorption edge data. Then a best fit of the sorption isotherm data was obtained by adjusting the equilibrium constant for the complexation with the weak sites. The best-fit parameters are shown in Table 2. Model predictions are superimposed with experimental data in Fig. 3a, and show that the obtained constants of cation exchange and strong site complexation reproduce the experimental data. The obtained constant of cation exchange and surface complexation at the strong site were fixed in the modelling of sorption isotherm data, the constant of surface complexation at the weak site were changed manually. As shown in Fig. 3b and c, the model fit the experimental data considerably well. At low Fe(II) concentration ($<10^{-8}$ M), the surface complexation at the strong site is the dominant process. At high Fe(II) concentration ($>10^{-8}$ M), the surface complexation at the weak site become the dominant reaction. At higher Fe(II) concentration ($>10^{-4}$ M), cation exchange reaction control the Fe(II) sorption.

However, there are some deficiency. At low Fe(II) concentration ($<10^{-8}$ M), a model with complexation constant value of 4.1 ± 0.2 for the strong site would best describe the sorption isotherm data at pH 5.0 ± 0.1. It is 2.9 ± 0.1 for sorption isotherm at pH 6.5 ± 0.1. While the best fit complexation constant value for the strong site is 3.4 ± 0.2 at the sorption edge. Finally in this model, the value that best fitting the sorption edge was applied. At high Fe(II) concentration ($>10^{-8}$ M), the best fit complexation constant is 0.8 ± 0.3 for weak site at pH 5.0 ± 0.1, while 1.4 ± 0.2 is the best fit for complexation constant at weak site at pH 6.5 ± 0.1. The surface complexation at weak site make small difference at the sorption edge at low concentration (10^{-7} M in this experiment). Taken into account the isotherm sorption at pH 5.5 ± 0.1, whose best fit weak site complexation constant is 1.6 ± 0.2, the value 1.4 ± 0.1 was chosen.

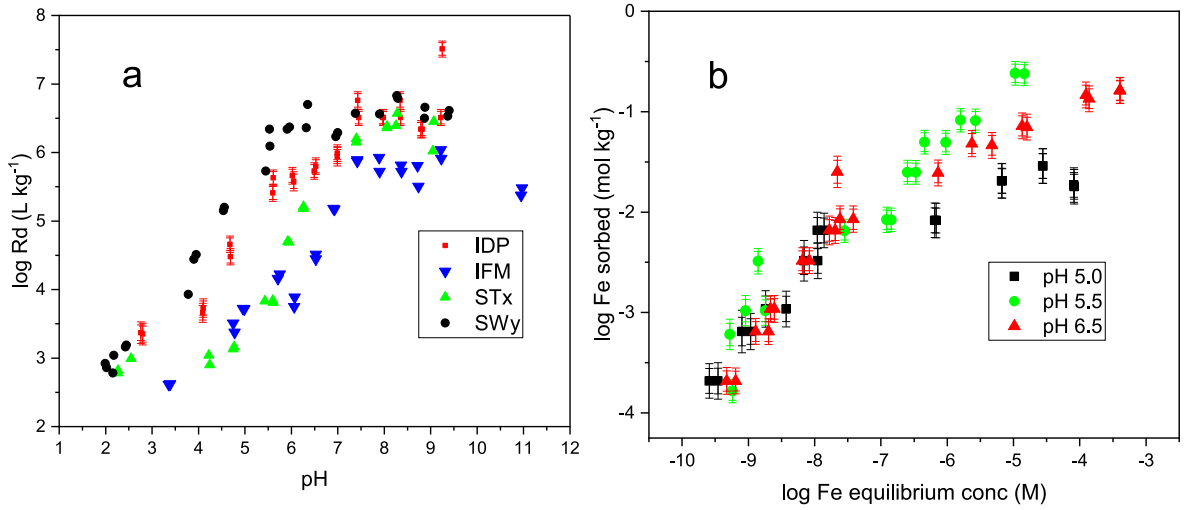

Fig. 1. Experimentally measured sorption edge on IDP, IFM (synthetic iron free montmorillonite), STx (the Texas montmorillonite) and SWy (the Wyoming montmorillonite). (a), and sorption isotherm at pH 5.0 ± 0.1, pH 5.5 ± 0.1 and pH 6.5 ± 0.1 on IDP(b), for Fe(II) in 0.1 M NaCl. The total Fe concentration in the sorption edge experiment is 1×10^{-7} M. Illite concentration is 1.2 g/L in the sorption isotherm Data on montmorillonite is from Soltermann et al. (2013, 2014a, 2014b).

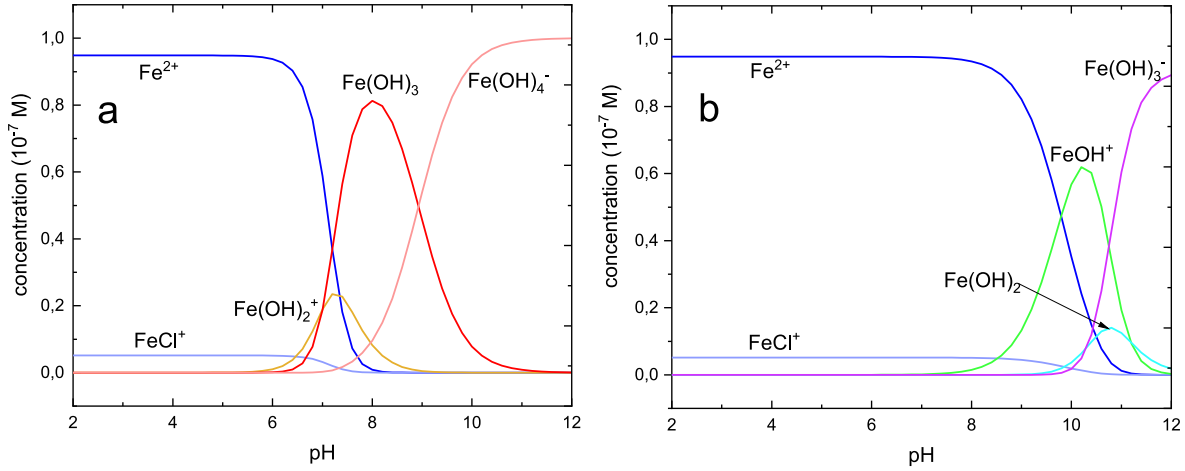

Fig. 2. Fe speciation calculated as a function of pH a) with and b) without redox potential consideration following equation (6) at 0.1 M NaCl background electrolyte. The total Fe concentration is 1×10^{-7} M.

Table 2
Fitted parameters of Fe(II) sorption on illite withsorption model, in which oxidation was not considered.

Cation exchange reaction	Log Kc
$2\ Na^+$–illite + $Fe^{2+} \leftrightarrow Fe^{2+}$–illite +$2\ Na^+$	2.0 ± 0.1
Surface complexation reactions	$Log^{S,W}K$
$\equiv S^SOH + Fe^{2+} \leftrightarrow \equiv S^SOFe^+ + H^+$	3.4 ± 0.2
$\equiv S^{W1}OH + Fe^{2+} \leftrightarrow \equiv S^{W1}OFe^+ + H^+$	1.4 ± 0.1

3.2. Sorption model B: Fe(II)/Fe(III) – illite interaction accounting for redox changes

As mentioned above, there are some flaw in sorption model A. Since the interfacial electron transfer was demonstrated to occur between aqueous Fe(II) and Fe-oxides, such as hematite, goethite, ferrihydrite and magnetite (Gorski and Scherer, 2009; Handler et al., 2009; Larese-Casanova and Scherer, 2007; Pedersen et al., 2005; Williams and Scherer, 2004; Yanina and Rosso, 2008). Furthermore, direct spectroscopic evidence was shown previously for the reduction of structural Fe(III) in a Fe-bearing smectite clay mineral (NAu-2, nontronite) by sorbed Fe(II) (Schaefer et al., 2011). Fe(II) sorption on Texas montmorillonite (STx), whose structural Fe-content was ≤0.5 wt%, was proven to be consistent with the uptake behavior of other divalent transition metals. While much more sorbed Fe was observed on Wyoming montmorillonite, the sorption model was modified by taking a simple surface oxidation reaction of sorbed Fe(II) on edge sites into account, as shown in equation (4) (see details in Text S1). In this concept, the aqueous Fe(II) is first sorbed on the amphoteric edge sites (strong and weak site) and then undergoes an oxidation by structural Fe (III) (Soltermann et al., 2014a).

$$\equiv S^{S,W1,W2}OH + Fe^{2+} \leftrightarrow \equiv S^{S,W1,W2}OFe^{2+} + H^+ + e^-$$

The reaction equilibrium constant is defined as:

$$K_{Fe3+} = \frac{\left[S^{S,W1,W2}OFe^{2+}\right]\cdot\{H^+\}\cdot\{e^-\}}{\left[\equiv S^{S,W1,W2}OH\right]\cdot\{Fe^{2+}\}} \quad (4)$$

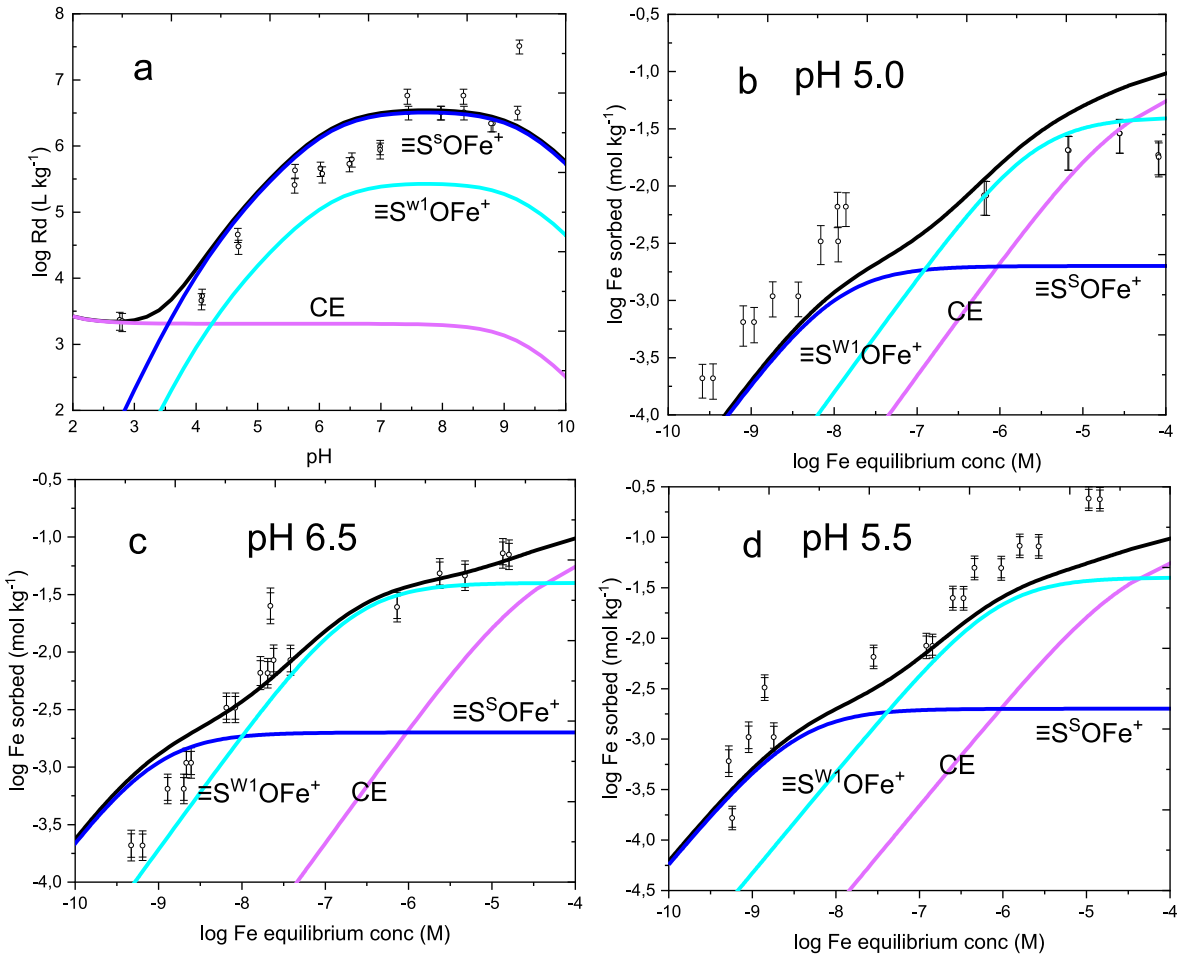

Fig. 3. Fitting results of Fe(II) sorption on illite in sorption modle A, a) edge at Fe_{tot} 1×10^{-7} M; b) isotherm at pH 5.0 ± 0.1; c) isotherm at pH 6.5 ± 0.1; d) isotherm at pH 5.5 ± 0.1; 0.1 M NaCl was used as background electrolyte. Black line is the total sorption (that is total log Rd or total log adsorbed Fe). Purple line represents the cation exchange sorption. Blue and cyan blue represents strong and weak site complexation species, respectively.

The common convention of the electron activity, pe = -log{e} is used in PHREEQC to represent the redox state of the solution, which could be calculated from Eh with equation (5).

$$pe = 16.9Eh\ (V) \text{ at } 25\ ^\circ C \tag{5}$$

$$Eh\ (V) = -(0.031 \pm 0.002)\ pH + (0.483 \pm 0.009)$$

$$R^2 = 0.93 \tag{6}$$

The redox potential Eh is assumed to vary with pH. Because the concentration of Fe in the edge sorption experiments was too low, it was not possible to perform accurate Eh measurements with a Pt-ring redox electrode. The relationship of Eh and pH was found to be linear in a montmorillonite suspension as shown in equation (6) (Soltermann et al., 2014a). Because illite has a similar structure as montmorillonite and a significant amount of Fe(III) is present in purified Na-illite (Bradbury and Baeyens, 2009a; Murad and Wagner, 1994), a similar behavior is expected in illite. Thus, the sorption model B modified with the oxidation of surface complexation. Since no reaction constants for iron free or low iron content illite are available, these constants for montmorillonite were used in this study on illite.

As shown in Fig. 2b, at a pH above 6, the oxidized Fe reacts with water and mainly forms $Fe(OH)_3$ and $Fe(OH)_4^-$. In this case, the model is extended with oxidized surface complexes further reacting with water. equations (7) and (8) are the total reactions. It includes three reactions: Fe^{2+} complexation with a surface site, oxidation of surface complexed Fe^{2+} by an interfacial electron transfer to surface complexed Fe^{3+}, and a reaction of the surface complexed Fe^{3+} with water.

$$\equiv S^SOH + Fe^{2+} + 3H_2O \leftrightarrow \equiv S^SOFe(OH)_3^- + 4H^+ + e^-$$

$$K_{Fe(OH)3} = \frac{\left[S^SOFe(OH)_3^-\right] \cdot \{H^+\}^4 \cdot \{e^-\}}{\left[\equiv S^SOH\right] \cdot \{Fe^{2+}\}} \tag{7}$$

$$\equiv S^SOH + Fe^{2+} + 4H_2O \leftrightarrow \equiv S^SOFe(OH)_4^{2-} + 5H^+ + e^-$$

$$K_{Fe(OH)4} = \frac{\left[S^SOFe(OH)_4^{2-}\right] \cdot \{H^+\}^5 \cdot \{e^-\}}{\left[\equiv S^SOH\right] \cdot \{Fe^{2+}\}} \tag{8}$$

The best fit results of the modelling are shown in Table 3 and Fig. 4.

Table 3
Best fit parameters of the modified sorption model for illite with oxidative Fe(II) uptake.

Cation exchange reaction	Log Kc
2 Na^+–illite + Fe^{2+} ↔ Fe^{2+}–illite + 2 Na^+	2.0 ± 0.1
Surface complexation reactions	$Log^{S,W}K$
$\equiv S^SOH + Fe^{2+} \leftrightarrow \equiv S^SOFe^+ + H^+$	1.9 ± 0.3
$\equiv S^{W1}OH + Fe^{2+} \leftrightarrow \equiv S^{W1}OFe^+ + H^+$	−1.7 ± 0.3
$\equiv S^SOH + Fe^{2+} \leftrightarrow \equiv S^SOFe^{2+} + H^+ + e^-$	−2.2 ± 0.3
$\equiv S^SOH + Fe^{2+} + 3H_2O \leftrightarrow \equiv S^SOFe(OH)_3^- + 4H^+ + e^-$	−22.0 ± 0.3
$\equiv S^SOH + Fe^{2+} + 4H_2O \leftrightarrow \equiv S^SOFe(OH)_4^{2-} + 5H^+ + e^-$	−31.5 ± 0.2
$\equiv S^{W1}OH + Fe^{2+} \leftrightarrow \equiv S^{W1}OFe^{2+} + H^+ + e^-$	−4.0 ± 0.3

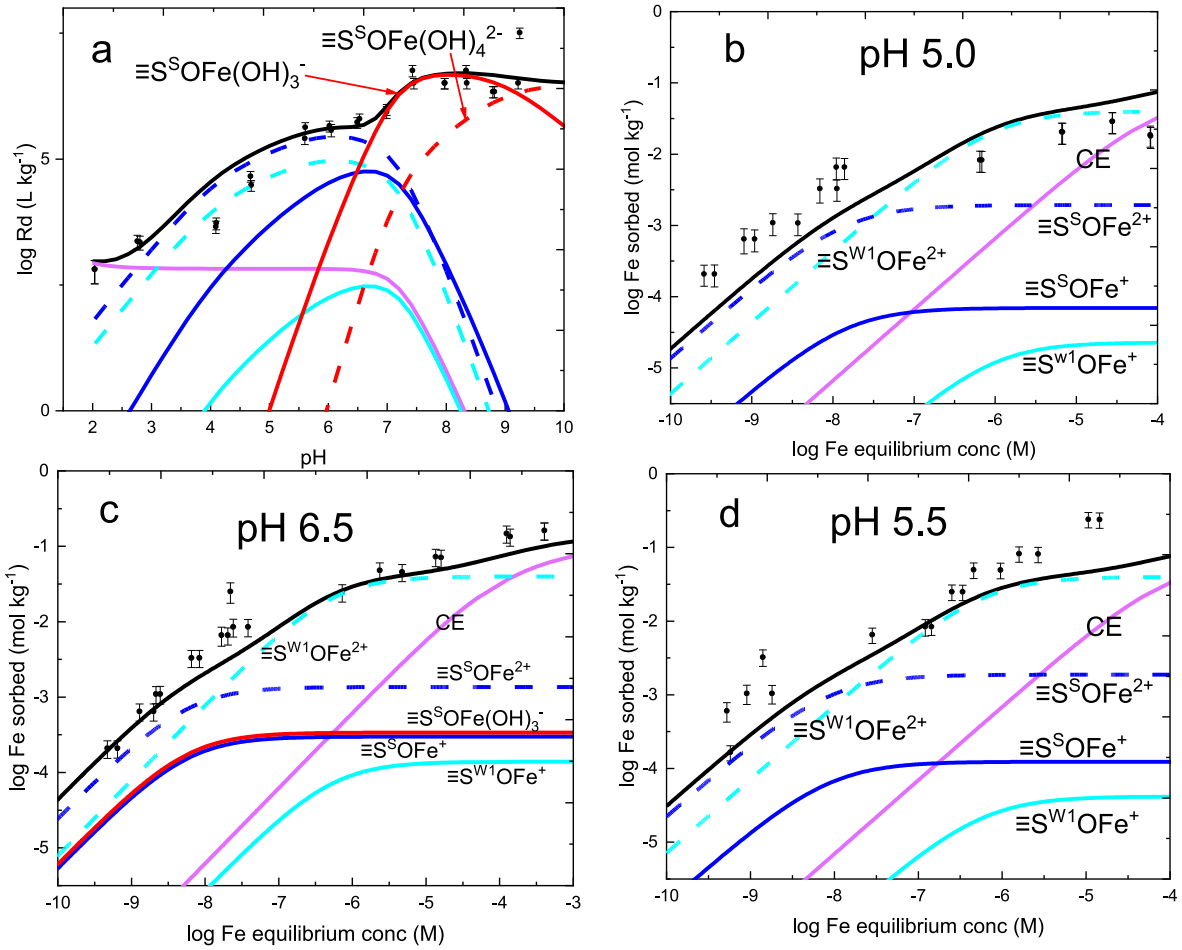

Fig. 4. Fit result of Fe(II) sorption on illite in sorption model B, a) edge at Fe_{tot} 1×10^{-7} M; b) isotherm at pH 5.0 ± 0.1; c) isotherm at pH 6.5 ± 0.1 and d) isotherm at pH 5.5 ± 0.1; 0.1 M NaCl was used as background electrolyte. Black line is the total sorption (that is total log Rd or total log adsorbed Fe).

Parameters previously obtained for STx do not reproduce the experimental data accurately enough (compare the blue and cyan solid line with the black experimental data points in Fig. 4a). So, the sorption model was modified with a surface oxidation reaction. It should be noted that in the modified model, the $\equiv S^{S}OFe^{2+}$ species sharply decreased from about pH 6 as shown in Fig. 4a, which is consistent with Fe(II) being oxidized and forming hydroxide Fe(III) species from pH 6 (Fig. 2b). In combination with the speciation of Fe at the same redox potential, two more species, $\equiv S^{S}OFe(OH)_3^-$ and $\equiv S^{S}OFe(OH)_4^{2-}$ were introduced with log K value of −22.0 and −31.5, respectively. In this model, the oxidized surface complex on the strong site is dominant in all experimental pH conditions studied, while oxidation of surface complex at weak site occurs only at pH below 7. At pH < 6.5, the oxidation of the surface complex ($\equiv S^{S}OFe^{+}$ and $\equiv S^{W1}OFe^{+}$) is the predominant reaction. While at pH 6–9, the oxidation is controlled by equation (7) and produce $\equiv S^{S}OFe(OH)_3^-$, whereas $\equiv S^{S}OFe(OH)_4^{2-}$ becomes the main species at pH above 9. On the other hand, at a low Fe(II) equilibrium concentration ($<10^{-8}$ M) at all experimental pH, most of the sorbed Fe(II) species ($\equiv SOFe^{+}$) was oxidized. With increasing Fe concentration, the weak site complex oxidation and cation exchange reaction gradually become the dominant sorption mechanism. There is also drawback in modelling. The sorption isotherm at low Fe(II) concentration especially at pH 5.0 ± 0.1 and pH 5.5 ± 0.1, a bigger values of the constant for the oxidation at strong site would fit the experimental better, which would result in an over estimation at low pH in the sorption edge. At high Fe(II) concentration, the underestimation of the data by the model can be explained by the formation of a Fe(III) precipitate (the saturation index is over 2.0 for hematite both at pH 5.5 ± 0.1 and 6.5 ± 0.1 at a Fe concentration above 10^{-5} M calculated from PHREEQC).

3.3. Sorption model C: extended model B including Fe precipitation

There could be another mechanism responsible for the seemingly high sorption of Fe at pH above 6 in the sorption edge. As shown in Fig. 2b, Fe(II) is gradually oxidized and forms Fe(III) species at pH 6.5 and more basic conditions. This may result in the formation of insoluble Fe(III) phases, for instance hematite, whose saturation index is higher than 2 at pH above 6.5. In this case, the measured Fe uptake from the solution could be explained by the precipitation of hematite. The modelling results considering hematite formation are shown in Fig. 5a (the red line represents sorption results from the contribution of a precipitate). The fitted parameters are the same as to sorption model B (Table 3), except reactions for forming $\equiv SOFe(OH)_3^-$, and $\equiv SOFe(OH)_4^{2-}$ are removed from this model. Similar as above, the fitted $\equiv SOFe^{2+}$ species sharply decrease from about pH 6 as shown in Fig. 5a (blue and cyan line). With the contribution of a hematite precipitate, the fitted log R_d values are perfectly consistent with experimental data. In the model, the oxidation of strong site and weak site surface complex is dominant at pH below 6 at low Fe(II) equilibrium concentration ($<10^{-7}$ M). Then the aqueous Fe(II) oxidizes from pH 6, and a precipitate is formed from then. However it is worth to notice that if a precipitate occurs above pH 6, such as 6.5, the equilibrium concentration of Fe in the solution should be constant once it reach the saturation concentration. However, a varying aqueous Fe(II) concentration was observed in the sorption isotherm at

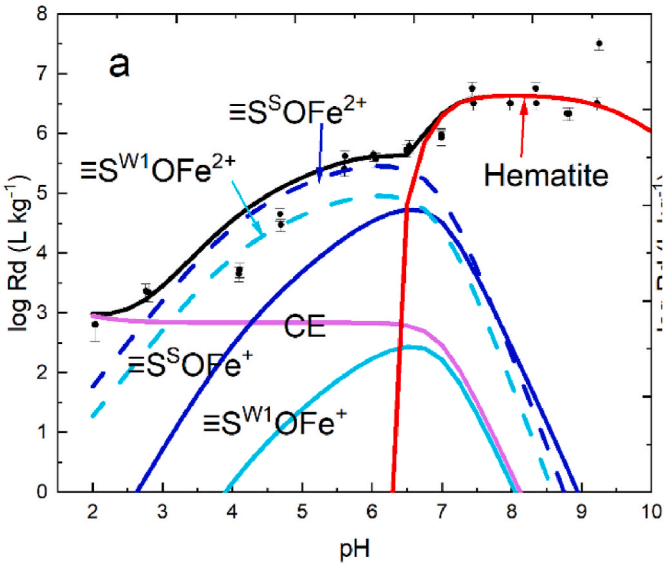

Fig. 5. Fit result of Fe(II) sorption edge on illite in model modified with a) hematite and surface oxidation; 0.1 M NaCl was used as background electrolyte. Hematite allowed to precipitate if with saturation index exceeds 2.0. Black line is the total sorption (that is total log Rd or total log adsorbed Fe).

pH 6.5 ± 0.1, so the precipitate does not control the aqueous concentrations. Either the precipitate is induced by surface site, so the process is not controlled by saturation concentration.

Detailed solids characterization would be helpful to further verify whether oxidation, precipitation or both are occurred on the surface. In this work, no iron hydro-oxides or iron oxides precipitate was observed by XRD measurements on samples at pH 8.68, pH 6.86 with 10^{-7} M Fe and at pH 6.5 with 2×10^{-4} M Fe(II) (see Supporting Information Fig. S2). So, the presence of a Fe-precipitate is not confirmed by XRD measurements. Still, the formation of an amorphous precipitate could not be excluded. Therefore, more spectroscopic investigations would be necessary and are of great interest to validate the exact sorption mechanism.

4. Conclusion

Fe(II) sorption edge and sorption isotherm measurements on illite were carried out using the batch sorption technique. The uptake of Fe(II) by illite could be successfully, to a certain extent, reproduced using the 2 SPNE SC/CE (2 sites protolysis non-electrostatic surface complex/cation exchange) sorption model (Model A). According to the obtained results, surface complexation at strong site is dominant at low Fe(II) concentration, while complexation at weak site and cation exchange at planar site become dominant at high Fe(II) concentration. Further improvement of the model was made by including oxidation of Fe(II) surface complexes (Model B) and surface precipitation were also discussed (Model C). The modified model was validated against available experimental data to some extent since the parameters used in the modified model are taken from iron free montmorillonite. Sorption experimental data on low iron content illite is need to validate the models. Although both surface precipitation (Model C) and oxidation of surface complexes (Model B) could improve representation of the experimental data compared to the model A, neither of the models perfectly reproduce data at all the condition studied. Therefore, further spectroscopic characterization of the solid phases would be necessary to verify whether oxidation or precipitate or both are occurred on the surface.

In spite of the uncertain mechanism at high pH, the sorption of Fe(II) at pH below 6.5 is unequivocal with most surface complexes being oxidized to $\equiv S^{S}OFe^{2+}$ at low Fe concentration, and to $\equiv S^{W1}OFe^{2+}$ at high Fe concentration. Its reactions and correspond equilibrium constant could be used to couple with redox sensitive rediaonuclides in the safety assessment of repository.

Declaration of competing interest

The authors declare that they have no known competing financial interests or personal relationships that could have appeared to influence the work reported in this paper.

Acknowledgements

This research is financially supported by the China Scholarship Council (CSC). The sorption experiments were carried out in Paul Scherrer Institut, Laboratory for Waste Management. The XRD measurement was performed in Institute of Geological science, University of Bern. we are grateful to all the colleagues and technicians, who helped us a lot in doing experiments and modelling.

Appendix A. Supplementary data

Supplementary data to this article can be found online at https://doi.org/10.1016/j.apgeochem.2022.105389.

References

Aeschbacher, M., Sander, M., Schwarzenbach, R.P., 2010. Novel electrochemical approach to assess the redox properties of humic substances. Environ. Sci. Technol. 44, 87–93. https://doi.org/10.1021/es902627p.

Altmann, S., 2008. 'Geo'chemical research: a key building block for nuclear waste disposal safety cases. J. Contam. Hydrol. 102, 174–179. https://doi.org/10.1016/j.jconhyd.2008.09.012.

Andra, 2005. Dossier 2005 Argile: Safety Evaluation of a Geological Repository.

Baeyens, B., Bradbury, M.H., 1997. A mechanistic description of Ni and Zn sorption on Na-montmorillonite Part I: titration and sorption measurements. J. Contam. Hydrol. 27, 199–222. https://doi.org/10.1016/S0169-7722(97)00008-9.

Baeyens, B., Bradbury, M.H., 2004. Cation exchange capacity measurements on illite using the sodium and cesium isotope dilution technique: effects of the index cation, electrolyte concentration and competition: modeling. Clay Clay Miner. 52, 421–431. https://doi.org/10.1346/CCMN.2004.0520403.

Baeyens, B., Maes, A., Cremers, A., Henrion, P.N., 1985. In situ physico-chemical characterisation of Boom clay. Radioact. Waste Manag. Nucl. Fuel Cycle 6, 391–408.

Bradbury, M., Baeyens, B., 2002. Sorption of Eu on Na-and Ca-montmorillonites: experimental investigations and modelling with cation exchange and surface complexation. Geochem. Cosmochim. Acta 66, 2325–2334. https://doi.org/10.1016/S0016-7037(02)00841-4.

Bradbury, M., Baeyens, B., 2009a. Sorption modelling on illite Part I: titration measurements and the sorption of Ni, Co, Eu and Sn. Geochem. Cosmochim. Acta 73, 990–1003. https://doi.org/10.1016/j.gca.2008.11.017.

Bradbury, M., Baeyens, B., 2009b. Sorption modelling on illite. Part II: actinide sorption and linear free energy relationships. Geochem. Cosmochim. Acta 73, 1004–1013. https://doi.org/10.1016/j.gca.2008.11.016.

Bradbury, M., Baeyens, B., Geckeis, H., Rabung, T., 2005. Sorption of Eu (III)/Cm (III) on Ca-montmorillonite and Na-illite. Part 2: surface complexation modelling. Geochem. Cosmochim. Acta 69, 5403–5412. https://doi.org/10.1016/j.gca.2005.06.031.

Bradbury, M.H., Baeyens, B., 1997. A mechanistic description of Ni and Zn sorption on Na-montmorillonite Part II: modelling. J. Contam. Hydrol. 27, 223–248. https://doi.org/10.1016/S0169-7722(97)00007-7.

Bradbury, M.H., Baeyens, B., 1999. Modelling the sorption of Zn and Ni on Ca-montmorillonite. Geochem. Cosmochim. Acta 63, 325–336. https://doi.org/10.1016/S0016-7037(98)00281-6.

Bradbury, M.H., Baeyens, B., 2005. Modelling the sorption of Mn (II), Co (II), Ni (II), Zn (II), Cd (II), Eu (III), Am (III), Sn (IV), Th (IV), Np (V) and U (VI) on montmorillonite: linear free energy relationships and estimates of surface binding constants for some selected heavy metals and actinides. Geochem. Cosmochim. Acta 69, 875–892. https://doi.org/10.1016/j.gca.2004.07.020.

Bradbury, M.H., Baeyens, B., 2006. Modelling sorption data for the actinides Am (III), Np (V) and Pa (V) on montmorillonite. Radiochim. Acta 94, 619–625. https://doi.org/10.1524/ract.2006.94.9-11.619.

Bradbury, M.H., Baeyens, B., 2011. Predictive sorption modelling of Ni (II), Co (II), Eu (IIII), Th (IV) and U (VI) on MX-80 bentonite and Opalinus Clay: a "bottom-up" approach. Appl. Clay Sci. 52, 27–33. https://doi.org/10.1016/j.clay.2011.01.022.

Brookshaw, D.R., Pattrick, R.A., Bots, P., Law, G.T., Lloyd, J.R., Mosselmans, J.F.W., Vaughan, D.J., Dardenne, K., Morris, K., 2015. Redox interactions of Tc (VII), U (VI), and Np (V) with microbially reduced biotite and chlorite. Environ. Sci. Technol. 49, 13139–13148. https://doi.org/10.1021/acs.est.5b03463.

De Cannière, P., Maes, A., Williams, S., Bruggeman, C., Beauwens, T., Maes, N., Cowper, M., 2010. Behaviour of Selenium in Boom Clay. External Report, SCK• CEN-ER-120.

Gabis, V., 1958. Etude préliminaire des argiles oligocènes du Puy-en-Velay (Haute-Loire). Bull. Mineral. 81, 183–185.

Gaines Jr., George L., Thomas, Henry C., 1953. Adsorption studies on clay minerals. II. A formulation of the thermodynamics of exchange adsorption. J. Chem. Phys. 21 (4), 714–718.

Glaus, M.A., Frick, S., Rossé, R., Van Loon, L.R., 2010. Comparative study of tracer diffusion of HTO, 22Na+ and 36Cl− in compacted kaolinite, illite and montmorillonite. Geochem. Cosmochim. Acta 74, 1999–2010. https://doi.org/10.1016/j.gca.2010.01.010.

Gorski, C.A., Klüpfel, L., Voegelin, A., Sander, M., Hofstetter, T.B., 2012. Redox properties of structural Fe in clay minerals. 2. Electrochemical and spectroscopic characterization of electron transfer irreversibility in ferruginous smectite, SWa-1. Environ. Sci. Technol. 46, 9369–9377. https://doi.org/10.1021/es302014u.

Gorski, C.A., Klüpfel, L.E., Voegelin, A., Sander, M., Hofstetter, T.B., 2013. Redox properties of structural Fe in clay minerals: 3. Relationships between smectite redox and structural properties. Environ. Sci. Technol. 47, 13477–13485. https://doi.org/10.1021/es403824x.

Gorski, C.A., Scherer, M.M., 2009. Influence of magnetite stoichiometry on FeII uptake and nitrobenzene reduction. Environ. Sci. Technol. 43, 3675–3680. https://doi.org/10.1021/es803613a.

Handler, R.M., Beard, B.L., Johnson, C.M., Scherer, M.M., 2009. Atom exchange between aqueous Fe (II) and goethite: an Fe isotope tracer study. Environ. Sci. Technol. 43, 1102–1107. https://doi.org/10.1021/es802402m.

Hofstetter, T.B., Neumann, A., Schwarzenbach, R.P., 2006. Reduction of nitroaromatic compounds by Fe (II) species associated with iron-rich smectites. Environ. Sci. Technol. 40, 235–242. https://doi.org/10.1021/es0515147.

Jaisi, D.P., Dong, H., Morton, J.P., 2008. Partitioning of Fe (II) in reduced nontronite (NAu-2) to reactive sites: reactivity in terms of Tc (VII) reduction. Clay Clay Miner. 56, 175–189. https://doi.org/10.1346/CCMN.2008.0560204.

Jaisi, D.P., Dong, H., Plymale, A.E., Fredrickson, J.K., Zachara, J.M., Heald, S., Liu, C., 2009. Reduction and long-term immobilization of technetium by Fe (II) associated with clay mineral nontronite. Chem. Geol. 264, 127–138. https://doi.org/10.1016/j.chemgeo.2009.02.018.

Jaisi, D.P., Kukkadapu, R.K., Eberl, D.D., Dong, H., 2005. Control of Fe (III) site occupancy on the rate and extent of microbial reduction of Fe (III) in nontronite. Geochem. Cosmochim. Acta 69, 5429–5440. https://doi.org/10.1016/j.gca.2005.07.008.

Keeling, J.L., Raven, M.D., Gates, W.P., 2000. Geology and characterization of two hydrothermal nontronites from weathered metamorphic rocks at the Uley graphite mine, South Australia. Clay Clay Miner. 48, 537–548.

Kefas, H.M., Patrick, D.O., Chiroma, T.M., 2007. Characterization of mayo-belwa clay. Leonardo Electron. J. Pract. Technol. 6, 123–130.

Larese-Casanova, P., Scherer, M.M., 2007. Fe (II) sorption on hematite: new insights based on spectroscopic measurements. Environ. Sci. Technol. 41, 471–477. https://doi.org/10.1021/es0617035.

Latta, D.E., Neumann, A., Premaratne, W., Scherer, M.M., 2017. Fe (II)–Fe (III) electron transfer in a clay mineral with low Fe content. ACS Earth Space Chem. 1, 197–208. https://doi.org/10.1021/acsearthspacechem.7b00013.

Lázár, K., Máthé, Z., 2012. Claystone as a potential host rock for nuclear waste storage. In: Clay Minerals in Nature–Their Characterization, Modification and Application. InTech, 2012, pp. 55–80.

Ma, B., Charlet, L., Fernandez-Martinez, A., Kang, M., Madé, B., 2019. A review of the retention mechanisms of redox-sensitive radionuclides in multi-barrier systems. Appl. Geochem. 100, 414–431. https://doi.org/10.1016/j.apgeochem.2018.12.001.

McBeth, J., Lloyd, J., Law, G., Livens, F., Burke, I., Morris, K., 2011. Redox interactions of technetium with iron-bearing minerals. Mineral. Mag. 75, 2419–2430. https://doi.org/10.1180/minmag.2011.075.4.2419.

Mogyorosi, K., Dekany, I., Fendler, J., 2003. Preparation and characterization of clay mineral intercalated titanium dioxide nanoparticles. Langmuir 19, 2938–2946. https://doi.org/10.1021/la025969a.

Murad, E., Wagner, U., 1994. The Mössbauer spectrum of illite. Clay Miner. 29 (1), 1–10.

Nagra, 2002. Project Opalinus clay, demonstration of disposal feasibility forspent fuel, vitrified high-level waste and long-lived intermediate-levelwaste. Safety Rep. Tech. Rep. 2–5.

Nayak, P.S., Singh, B., 2007. Instrumental characterization of clay by XRF, XRD and FTIR. Bull. Mater. Sci. 30, 235–238.

Neumann, A., Olson, T.L., Scherer, M.M., 2013. Spectroscopic evidence for Fe (II)–Fe (III) electron transfer at clay mineral edge and basal sites. Environ. Sci. Technol. 47, 6969–6977. https://doi.org/10.1021/es304744v.

Nirond, Ondraf, 2001. Safety Assessment and Feasibility Interim Report 2, pp. 2001–2005 (Safir 2), Nirond.

Pedersen, H.D., Postma, D., Jakobsen, R., Larsen, O., 2005. Fast transformation of iron oxyhydroxides by the catalytic action of aqueous Fe (II). Geochem. Cosmochim. Acta 69, 3967–3977. https://doi.org/10.1016/j.gca.2005.03.016.

Peretyazhko, T., Zachara, J.M., Heald, S.M., Jeon, B.-H., Kukkadapu, R.K., Liu, C., Moore, D., Resch, C.T., 2008. Heterogeneous reduction of Tc (VII) by Fe (II) at the solid–water interface. Geochem. Cosmochim. Acta 72, 1521–1539. https://doi.org/10.1016/j.gca.2008.01.004.

Poinssot, C., Baeyens, B., Bradbury, M.H., 1999. Experimental and modelling studies of caesium sorption on illite. Geochem. Cosmochim. Acta 63, 3217–3227. https://doi.org/10.1016/S0016-7037(99)00246-X.

Schaefer, M.V., Gorski, C.A., Scherer, M.M., 2011. Spectroscopic evidence for interfacial Fe (II)− Fe (III) electron transfer in a clay mineral. Environ. Sci. Technol. 45, 540–545. https://doi.org/10.1021/es102560m.

Soltermann, D., Baeyens, B., Bradbury, M.H., Marques Fernandes, M., 2014a. Fe (II) uptake on natural montmorillonites. II. Surface complexation modeling. Environ. Sci. Technol. 48, 8698–8705. https://doi.org/10.1021/es501902f.

Soltermann, D., Marques Fernandes, M., Baeyens, B., Dähn, R., Miehé-Brendlé, J., Wehrli, B., Bradbury, M.H., 2013. Fe (II) sorption on a synthetic montmorillonite. A combined macroscopic and spectroscopic study. Environ. Sci. Technol. 47, 6978–6986. https://doi.org/10.1021/es304270c.

Soltermann, D., Marques Fernandes, M., Baeyens, B., Dähn, R., Joshi, P.A., Scheinost, A. C., Gorski, C.A., 2014b. Fe (II) uptake on natural montmorillonites. I. Macroscopic and spectroscopic characterization. Environ. Sci. Technol. 48, 8688–8697. https://doi.org/10.1021/es501887q.

Tsarev, S., Waite, T.D., Collins, R.N., 2016. Uranium reduction by Fe (II) in the presence of montmorillonite and nontronite. Environ. Sci. Technol. 50, 8223–8230. https://doi.org/10.1021/acs.est.6b02000.

Williams, A.G., Scherer, M.M., 2004. Spectroscopic evidence for Fe (II)− Fe (III) electron transfer at the iron oxide− water interface. Environ. Sci. Technol. 38, 4782–4790. https://doi.org/10.1021/es049373g.

Yanina, S.V., Rosso, K.M., 2008. Linked reactivity at mineral-water interfaces through bulk crystal conduction. Science 320, 218–222. https://doi.org/10.1126/science.1154833.